Evaluation of Creep Crack Growth Criteria for IN-100 at Elevated Temperature

T. D. Hinnerichs*
U. S. Air Force Weapons Laboratory, Kirtland AFB, New Mexico
A. N. Palazotto†
Air Force Institute of Technology, Wright-Patterson AFB, Ohio
and
T. Nicholas‡
Air Force Wright Aeronautical Laboratories, Wright-Patterson AFB, Ohio

Seven crack growth rate criteria from numerical computations of simulated creep crack growth experiments are evaluated. A finite element computer program is utilized to calculate the various parameters. Both near-field, or local, as well as far-field criteria are examined. The results indicate that environment plays a major role in crack growth in a nickel-base superalloy, IN-100, at 732°C and that time effects must be considered in modeling crack growth using local criteria. Stress intensity and net-section stress are found to be adequate as correlating parameters but are unable to model observed transient phenomena.

I. Introduction

THE U.S. Air Force currently places strict fracture mechanics based requirements on airframe construction and maintenance. These requirements involve prediction of the remaining useful life of a structural component through specified fracture mechanics techniques and the detection of flaws by periodic nondestructive inspection. Consequently, if an airframe part is examined and found to have no flaws that can grow to critical size prior to the next periodic inspection, it can be returned to service.

In contrast to the airframe, low-cycle-fatigue limited jet engine parts are retired from service when their design life has been reached even though no flaws have yet been found in most of them. This situation occurs because the retirement of engine disks is based on a "crack initiation" criterion. Under this criterion, all components of a given population are considered to have no remaining service life as soon as a measurable crack, typically of the order of 1 mm or less, has formed in the member of the population which has statistical minimum strength properties.[1] No attempt is made to utilize the additional life associated with the remaining members of the population which have statistically longer lives and are therefore expected to be uncracked, or have cracks smaller than the detectable size.

From a safety standpoint, this approach has been generally very successful. However, for real materials and real design situations, lifetimes based on time to crack initiation of the minimum member tend to be extremely conservative. With increasing replacement costs for components as well as the uncertainty of the availability of critical strategic materials in these parts, it is not surprising to find that alternative life management schemes are being considered. Retirement for cause based on a criterion which considers the fatigue crack propagation life based on a fracture mechanics approach is now being investigated for USAF engines. Under this philosophy, components are kept in service until a predetermined crack size is detected which will grow to catastrophic size in one or more inspection intervals. This approach to life management is critically dependent on not only reliable inspection techniques but on the ability to accurately predict the growth of a flaw under typical engine operating conditions.

Various parameters controlling the fatigue crack growth in engine components are strain, stress, stress intensity, temperature, load application frequency, and environment. The relative effects of each parameter are reviewed by Speidel,[2] who shows that at each elevated temperature there is a critical frequency below which the crack growth rate is creep dependent (i.e., dependent on exposure time to load), and this creep dependency increases with decreasing frequency. Also, the presence of an aggressive environment is another factor which results in a frequency dependence of the crack growth rate which is very similar to that brought about by creep.

Typical engine missions include, among other features, dwell times (hold times at constant stress) of the order of minutes at high stress levels. Crack growth is then influenced by parameters such as stress and strain levels, stress intensity, temperature, and environment because load cycling is not occurring during these dwell periods. In addition, high stress concentrations in the vicinity of the crack tip combined with the high temperature environment lead to nonlinear and time-dependent stress-strain behavior for the material. Thus, yielding is encountered in the vicinity of the crack tip within a plastic zone as well as time-dependent flow or creep. Finally, environmental factors such as temperature and atmosphere might affect the ductility of the material, thereby lowering the ability of the material to strain prior to fracture.

Two types of approaches can be utilized to predict crack growth behavior under creep conditions. In one case, far-field fracture mechanics parameters such as the stress intensity, C^* integral, or net-section stress can be used to correlate crack growth rate. In the second case, localized failure criteria such as stress or strain at the crack tip can be utilized to predict small increments of crack extension based on detailed stress analysis in the vicinity of the crack tip. In the present investigation, both types of crack growth criteria are evaluated based on a detailed finite element analysis of a center cracked geometry test specimen incorporating precise displacement measurements in creep crack growth experiments. The results provide a reliable numerical technique for determining crack growth rate for a particular material under creep conditions.

Presented as Paper 81-0540 at the AIAA/ASME/ASCE/AHS 22nd Structures, Structural Dynamics and Materials Conference, Atlanta, Ga., April 6-8, 1981; submitted April 14, 1981; revision received June 21, 1982.

*Section Chief of Structural Dynamics. Member AIAA.
†Professor, Aerospace Engineering. Associate Fellow AIAA.
‡Materials Research Engineer.

II. Approach

The analysis utilizes a two-dimensional (plane stress/plane strain) nonlinear, time-dependent, finite element program, referred to as VISCO,[3] to investigate creep crack growth under constant load. The finite element analysis incorporates constant-strain triangular elements, while the nonlinear time-dependent material constitutive model takes the form of the Bodner-Partom viscoplastic flow law.[4-7] This flow law is integrated through time by an Euler extrapolation scheme[8] and incorporated into the overall finite element program by means of the residual force method.[9] Material constants for the Bodner material model were determined by Stouffer[10] to best match the behavior of the test material, at the temperature at which all tests were conducted.[11] The test material is gatorized IN-100,® a nickel-base superalloy used for turbine disks in jet engines. The test temperature of 732°C (1350°F) was chosen as the upper bound of temperatures at which this material can be used without significant loss of modulus or yield strength and where time-dependent material behavior is observed.

Time step sizes of the Euler scheme are maximized subject to specified amounts of change in stress and strain over a given time step. This time step maximization scheme provides the ability to transition from time steps which are a small fraction of a second for the load up phase to large time steps of the order of minutes for the constant load creep phase. This variable time step capability is a necessity to make a numerical study of creep crack growth computationally feasible.

Crack growth and possible crack closure during unloading is accounted for by simple modifications to the structural stiffness matrix. These simple modifications are made possible by choosing an interactive Gauss-Siedel linear equation solver[12] which requires no explicit inversion of the stiffness matrix. Hence, between time steps, pertinent terms of the stiffness matrix easily can be changed to account for crack growth and the general procedure continued without costly matrix inversion time required.

The finite element program which has the capability of accounting for material creep and plasticity as well as for crack growth is used to study creep crack growth in a center cracked plate specimen. The specimens which are modeled have several different initial crack lengths with a node spacing of 20 μ near the crack tip and are subjected to various loads that are chosen to coincide with the geometries and loads used in a parallel experimental program. A complete description of the program and finite element models used in the analysis can be found in Ref. 3.

The analytical model is used to determine the actual rate of creep crack growth in test specimens from experimental displacement and compliance measurements. Both far- and near-field parameters are investigated to determine which ones are most applicable for predicting creep crack growth in a typical jet engine turbine disk alloy, IN-100, at 732°C. A hybrid experimental-numerical (HEN) procedure[13] is employed in which crack growth rates were determined from finite element model displacement results which are compared with experimental data for the same geometry and loading conditions. The specimen geometry is a center cracked panel 25.4 mm wide and 7.6 mm thick. Details of the experimental procedure are reported in Refs. 3 and 13. The crack is allowed to grow sufficiently by releasing nodes so that predicted crack opening displacement rates from the finite element model match experimental data for the same geometry and loading conditions. From these results, which provide good correlation of displacements between model and experiment, seven creep crack growth criteria are evaluated from the calculated parameters in the finite element scheme.

One of the tests of a parameter's ability to correlate or predict crack growth rates is its demonstrated applicability over a range of crack lengths, stress intensity levels, and specimen geometries. In this investigation, only a center cracked plate geometry is utilized, but both short and long crack lengths are used as well as a wide range of stress intensities from 17.9 to 40.4 MPa$\sqrt{\text{m}}$ which cover a range of crack growth rates of nearly two orders of magnitude. A summary of test conditions showing the range of K and initial crack lengths and an index of the computer runs is presented in Table 1. The columns labeled HEN and DAM ACC (damage accumulation) refer to the computer run numbers used for the determination of crack growth rates from the HEN procedure and evaluation of a critical damage accumulation criterion, respectively. The parameters used for the strain or crack opening displacement criteria in the computer runs are also presented and are discussed later.

III. Crack Growth Criteria

Both near- and far-field parameters are investigated in an attempt to identify which parameter can be used to predict or correlate crack growth rates. Near-field or local crack tip parameters such as strain or crack opening displacement (COD) have shown promise elsewhere for correlating finite element results with experimental crack growth data.[14,15] To use a near-field parameter, a numerical scheme is required to compute values of that parameter for application purposes. When a critical value is achieved, it can then be used as a criterion for local failure which allows nodes or elements in a finite-element scheme to be broken or released. Far-field parameters, on the other hand, are quantities which determine the rate at which the crack grows and provide a one-to-one correlation with growth rate. If the computation of the far-field parameter is strongly influenced by the growth rate itself, then correlation can be difficult to establish.

A. Critical Strain Criterion

The first local crack tip criterion examined is strain normal to the crack. Examination of the strains in the elements adjacent to the crack tip prior to each node release for crack growth in the HEN VISCO runs reveals that no single value for the critical strain would appear to satisfy all test conditions. However, a few VISCO runs were made using a fixed critical strain criterion to further evaluate its applicability.

The critical strain criterion is implemented in VISCO by comparing the average of the plastic strain components normal to the crack and within elements adjacent to the crack tip with a critical strain value, ϵ_{crit}, as time progresses. When the average crack tip plastic strain exceeds the critical value, ϵ_{crit}, the crack tip node is released and unloaded in 5 s. The 5-s

Table 1 Table of test conditions and computer runs

Test No.	$2a_0/w$	K, MPa$\sqrt{\text{m}}$	HEN	Computer runs ϵ_{crit}	Computer runs COD_{crit}, mm	Computer runs DAM ACC
8a	0.2734	17.9	S1	E1 0.030		D3
9	0.2734	40.4	S2	E2 0.075 E3 0.090	C1 1.27×10^{-3} C2 1.15×10^{-3}	D4
5	0.2734	27.5	S3			D1
12b	0.6234	32.4	S4			D6
12a	0.4734	19.2	S6			D5
6	0.4734	30.7				D2

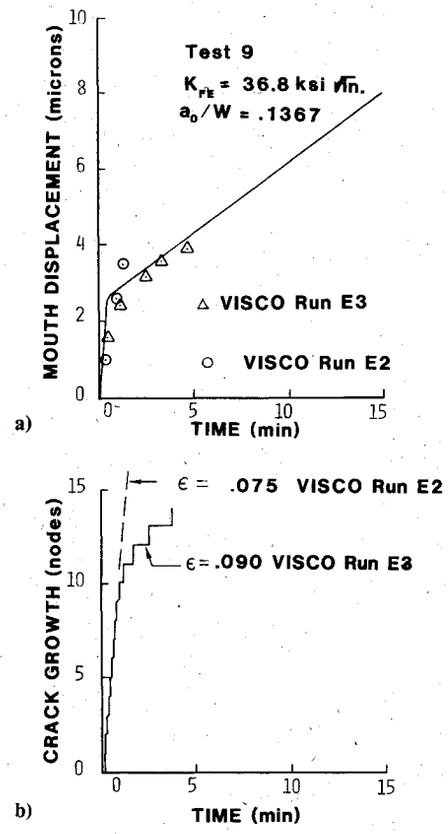

Fig. 1 Results of application of critical strain crack growth criterion, $K = 40.4$ MPa$\sqrt{\text{m}}$; a) displacements due to crack growth, b) crack growth.

release time is chosen to avoid transient effects of an instantaneous release method and was found previously to have no effect on the results for the crack growth rates encountered in these tests.[13] The results of the calculations using the critical strain criterion are summarized in Table 1. An ϵ_{crit} value of 0.030 is found to work well from the HEN VISCO runs of test 8a, where K is 17.9 MPa$\sqrt{\text{m}}$. However, for test 9, where K is 40.4 MPa$\sqrt{\text{m}}$, the value of ϵ_{crit} needs to be 0.090 to work well as shown in Fig. 1a (run E3). The corresponding ϵ_{crit} dependent crack growth vs time is given in Fig. 1b. A slightly smaller ϵ_{crit} value of 0.075 allows too much displacement compared to test data as seen in Fig. 1 for run E2. The displacement results for an ϵ_{crit} value of 0.090 appear to fit the data quite well over the first 5 min of the test. Likewise the resulting crack growth in Fig. 1b agrees quite well with the HEN VISCO data of run S2. However, the ϵ_{crit} value needed to match the data for test 9 is far greater than the value needed to match data in test 8a, where K is much smaller. Thus, no single value of critical strain appears to work as a failure criterion for the range of test conditions covered here.

To further illustrate this point, crack tip strain values taken at the time a crack tip node was to be released in the HEN VISCO runs are plotted as shown in Fig. 2. The abscissa, time, is the time from the beginning of each simulated crack growth test. This plot is constructed in an attempt to find a general trend of the critical strain values or to determine a mathematical relationship with time to envelope the HEN results. In general the strains are high for short times, or as the first few nodes are released, and then diminish with time to a common value of approximately 0.03. The values at the upper part of the envelope in Fig. 2 represent those obtained in tests involving the upper range of growth rates and K values covered in this investigation. The lower part of the envelope represents the slower growth rates or lower K values. In order to develop a critical strain functional expression, one can see

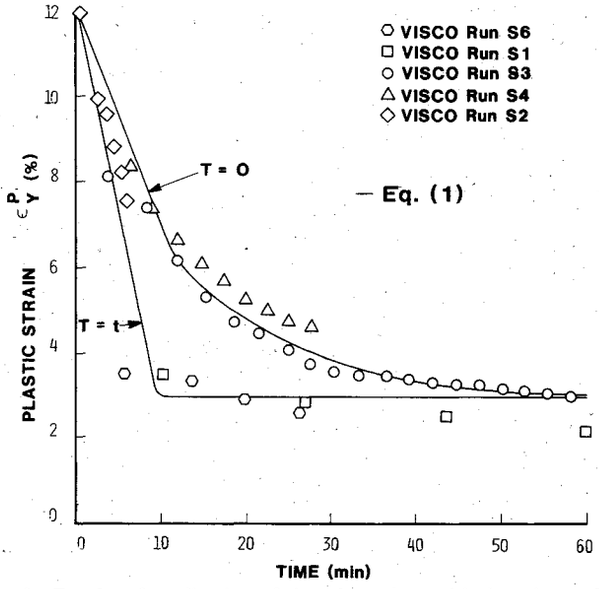

Fig. 2 Results of application of time-dependent critical strain crack growth criterion.

from the plot a need for a parameter, which decays with total test time, which would fit the upper bound strain values in Fig. 2 related to rapid crack growth. In addition, for the lower range of crack growth rates, the expression must have the capability of allowing the region around the crack tip node to deteriorate with exposure to the crack tip environment (i.e., not only the environment external to the specimen but also the singular strain state internal to the specimen). This additional crack tip deterioration is considered to be displayed by the lower bound of strain values in Fig. 2 which corresponds to the lowest crack growth rates. To construct a general expression which decays with test time, a negative exponential function is employed. Furthermore, because critical strain values appear to diminish additionally with long crack tip exposure time, but not as rapidly as an exponential function would dictate, a cosine function is used.

An empirical expression for the critical strain that fits the HEN VISCO results fairly well is given by

$$\epsilon_{crit} = \epsilon_0 [A\exp(-bt)\cos(\pi T/2T_0) + 1] \quad \text{if} \quad T \le T_0$$
$$= \epsilon_0 \quad \text{if} \quad T > T_0 \qquad (1)$$

where $\epsilon_0 = 0.03$, $A = 3.0$, $b = 1.34 \times 10^{-3}$ s^{-1}, $T_0 = 600$ s. Times t and T refer to total test time and crack tip exposure time, respectively. The value of ϵ_0 represents the critical strain for large time. The coefficient A is determined at t equal to zero. Once A and ϵ_0 are chosen, b is determined by best fitting the upper bound where crack tip exposure time is small and set equal to zero (i.e., $T = 0$). The parameter T_0 determines how rapidly the critical strain diminishes to ϵ_0 with crack tip exposure time T.

Motivation for the development of Eq. (1) comes from consideration of environmental effects such as oxidation at these high temperatures from exposure to laboratory air. The oxidation is associated with changing material properties at the crack tip such as the critical strain value. Crack growth in alloys similar to IN-100 has been found to be quite sensitive to the environment and the resulting oxidation that can occur when an elevated temperature crack growth test is done in air.[16] Therefore Eq. (1) is an attempt to represent the rate at which the critical strain for crack growth is diminished with time due to environmental effects. No computer runs are made, however, utilizing this criterion. It could be employed in VISCO in the following steps.

1) Record both total test simulation time t and crack tip exposure time T.

2) Evaluate the critical strain level during each time step from Eq. (1).

3) Compare with the crack tip element's plastic strain accumulating in the VISCO analysis.

4) Release the crack tip node when the VISCO plastic strain at the crack tip exceeds ϵ_{crit} from Eq. (1).

5) Crack tip exposure time T is set to zero and the foregoing steps 1-4 are repeated for the next crack tip node.

B. Critical Crack Opening Displacement Criterion

The crack opening displacement (COD) is defined here as the COD at the first node behind the crack tip in the finite element model. Examination of CODs from HEN VISCO runs just prior to releasing a crack tip node reveals that no single COD value can be used for all test conditions as a critical COD. A value of 7.11×10^{-4} mm is found from HEN VISCO results for test 8a with $K=17.9$ MPa$\sqrt{\text{m}}$ to work best. A few VISCO runs, summarized in Table 1, are performed with a critical COD criterion for test 9 which has a larger value of $K=40.4$ MPa$\sqrt{\text{m}}$. For this case, the best value of a critical COD is approximately 1.27×10^{-3} mm, which is nearly double the value observed in test 8a for the much lower K value. The results of the calculations for test 9 are presented in Fig. 3 which shows that the results are very sensitive to small changes in critical COD. Therefore further evaluation of this criterion is deemed unnecessary as compared with the less sensitive critical strain criterion.

C. Critical Damage Accumulation Criterion

In several theoretical works, including those of Goodall and Chubb,[17] creep rupture of uncracked components under a varying stress history is governed by the life fraction rule. Consequently, for a uniaxial stress history, $\sigma(t)$, rupture occurs at a time t_r given by

$$\int_0^{t_r} \frac{dt}{t_r(\sigma)} = 1 \tag{2}$$

where $t_r(\sigma)$ is the rupture time corresponding to a constant stress level, σ. When experimental stress values are plotted against their rupture times on logarithmic scales, the relationship is often linear in the region of practical interest. Thus, if M and C are material constants, it is assumed that

$$\sigma^M t_r(\sigma) = C \tag{3}$$

Substituting Eq. (3) in Eq. (2) yields

$$\int_0^{t_r} \sigma^M dt = C \tag{4}$$

The description of creep rupture given by Eqs. (2-4), discussed by Goodall and Chubb, is only one of several possible formulations. However, neither experimental nor theoretical work has provided an alternative to Eq. (2) that gives a significantly better description of material response.

Although Eq. (3) applies most directly to creep rupture of uncracked uniaxial specimens, similar behavior might be expected in creep crack propagation. A schematic of the postulated behavior involved with creep crack propagation is given in Fig. 4, which shows a creep damage front preceding the crack. Within this front, the material is accumulating creep damage in the form of microcracks. This type of creep damage is also associated with creep rupture of uncracked components.

Equation (4) is applied as a crack growth criterion within a process zone, δ, as shown in Fig. 4, where large stresses producing creep are expected to occur. The rupture time is

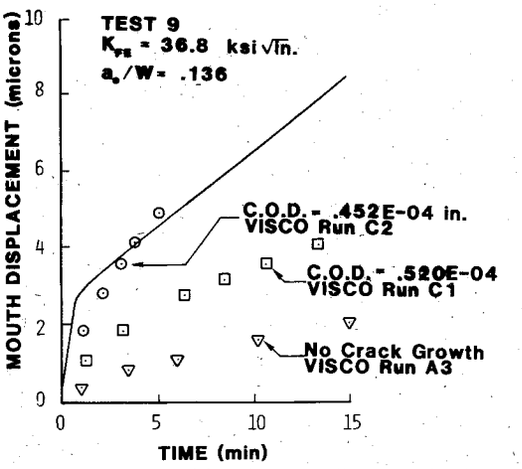

Fig. 3 Displacements resulting from application of critical COD criterion, $K=40.4$ MPa$\sqrt{\text{m}}$.

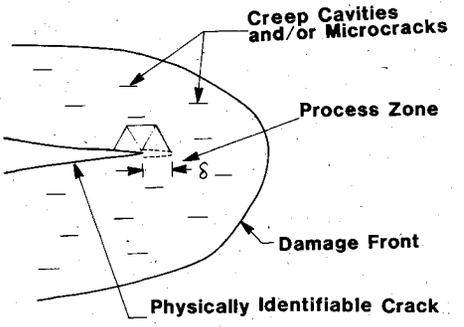

Fig. 4 Schematic representation of processes in creep crack propagation.

then redefined from Eq. (2) to be the elapsed time the crack requires to grow from one node, in the HEN VISCO results, to the next node. In other words, it is the time period during which the process zone δ is exposed to the crack tip stress field prior to rupture. In the VISCO finite element analysis, the dimension of the process zone is taken as the size of one element preceding the crack tip. The average component of stress normal to the crack from three elements adjacent to the crack tip is used as the stress, σ, in Eq. (4) as shown in Fig. 4.

Because the greatest stress exists at the crack tip and environmental degradation is considered to be most prevalent there, most damage accumulation is assumed to occur in the process zone after the arrival of the crack tip at the process zone's border. Therefore, time in Eq. (4) is measured from crack tip arrival time at the current tip node, t_A; thus

$$\int_{t_A}^{t_A+t_r} \sigma^M dt = C \tag{5}$$

The constants M and C are determined based on results from the HEN VISCO runs. To accomplish this, Eq. (5) is approximated by

$$\sigma_{av}^M t_r = C \tag{6}$$

The rupture times or crack growth times t_r are taken from HEN VISCO results. The stress, σ_{av}, also based on HEN results, is an average over time t_r of the crack tip stress defined previously. The intent here is to develop values for M and C which apply to the entire set of tests. It becomes obvious that there are more combinations of t_r and σ_{av} than necessary to uniquely define M and C. Consequently, to include the data from each HEN VISCO run, a least-squares fit of the time-stress data on a log-log plot is used to obtain

the best values of

$$M=15$$

$$C=2.31\times10^{112}(\text{MPa})^{15}\ \text{s}$$

Equation (5), together with the foregoing constants, are then incorporated into VISCO as a critical damage accumulation criterion for crack growth. Six VISCO computer runs using this crack growth criterion were conducted as summarized in Table 1.

Figures 5-7 present the reuslts of applying VISCO with the critical damage accumulation criterion to the indicated test number corresponding to an intermediate, minimum, and maximum K value from all the tests analyzed. The resulting VISCO displacements are compared to test data in Figs. 5a-7a, whereas the resulting crack growth from VISCO is given in Figs. 5b-7b. For the highest stress intensity value in test 9 in Fig. 7, the difference between test data and VISCO results is greatest. Part of this difference might be due to the fact that at this high load ($K=40.4$ MPa$\sqrt{\text{m}}$) the damage zone as indicated in Fig. 4 is much larger than the process zone used herein (i.e., one element size or a characteristic dimension of 1.98×10^{-2} mm). Hence significant damage accumulation can occur in the material before arrival of the crack tip or time t_A for a given element in the crack path. This damage occurring in an element prior to t_A for that respective element is neglected in the present damage accumulation criterion. For the intermediate K levels as shown in Fig. 5, agreement with the test data is quite good considering that creep rates for the same test conditions can easily vary by a factor of 2 or 3. For this reason log-log plots are normally used to plot creep data.[18] For the lowest K value, the agreement is fair as shown in Fig. 6. In this case, the displacement rate is predicted accurately after an initial overshoot in the early time period.

The M and C values used are determined from the approximate Eq. (6) expression. Crack growth results from this criterion might also be improved by iterating or making small changes to M and C and making further VISCO runs in an effort to better fit test data. An alternative method of evaluating a damage accumulation criterion would be to accumulate damage for all time and not just within the process zone. The results might be improved at the expense of increased computational time.

IV. Far-Field Crack Growth Rate Criteria

In addition to local criteria discussed above, several far-field crack growth rate criteria are considered based on numerical values of the steady-state crack growth rates obtained in the HEN VISCO runs. The steady-state crack growth rates are determined by best fitting a straight line to the crack growth curves. In most cases, the initial crack growth rate is higher than that achieved after several minutes as is the displacement rate (see Figs. 6 and 7). The initial transient portion of these crack growth curves is ignored when computing the steady-state values. In the following sections, several possible correlating parameters are discussed.

A. Stress Intensity Factor Criterion

Crack growth rate, $\dot{a}$, has previously been found to correlate with the elastic stress intensity factor in the form

$$\dot{a}=A(K)^n \tag{7}$$

This relationship is a straight line on log-log paper, as shown in Fig. 8. The experimental data represented by the line in Fig. 8 were obtained by Donat et al.[19] for IN-100 at 732°C, which is the same alloy and temperature used in the present investigation. Note that Donat's experimental data cover a range in K values from 33 to approximately 90 MPa$\sqrt{\text{m}}$. In

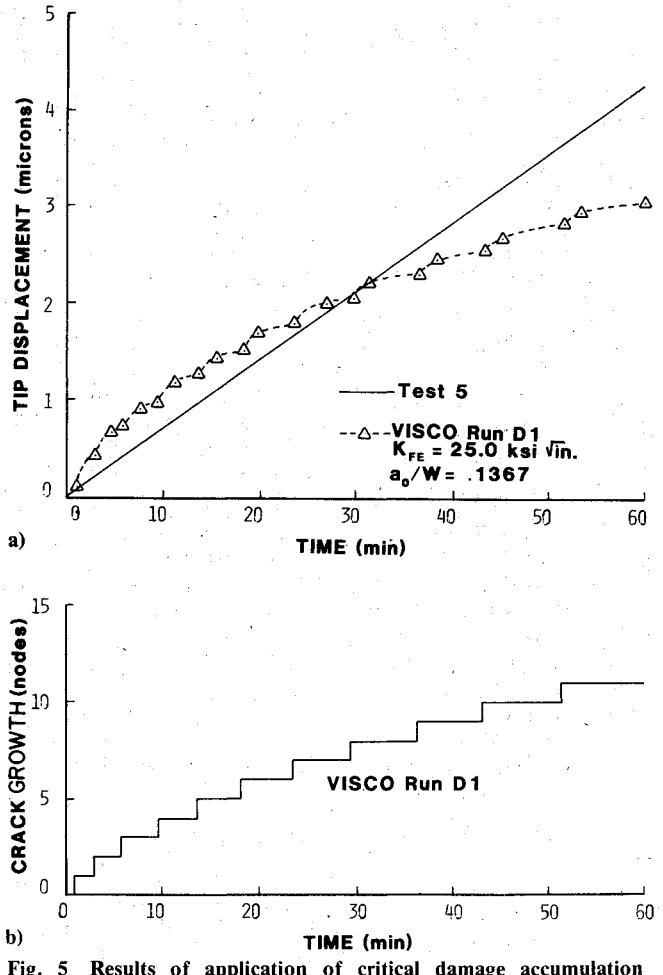

Fig. 5 Results of application of critical damage accumulation criterion, $K=27.5$ MPa$\sqrt{\text{m}}$; a) displacements, b) crack growth.

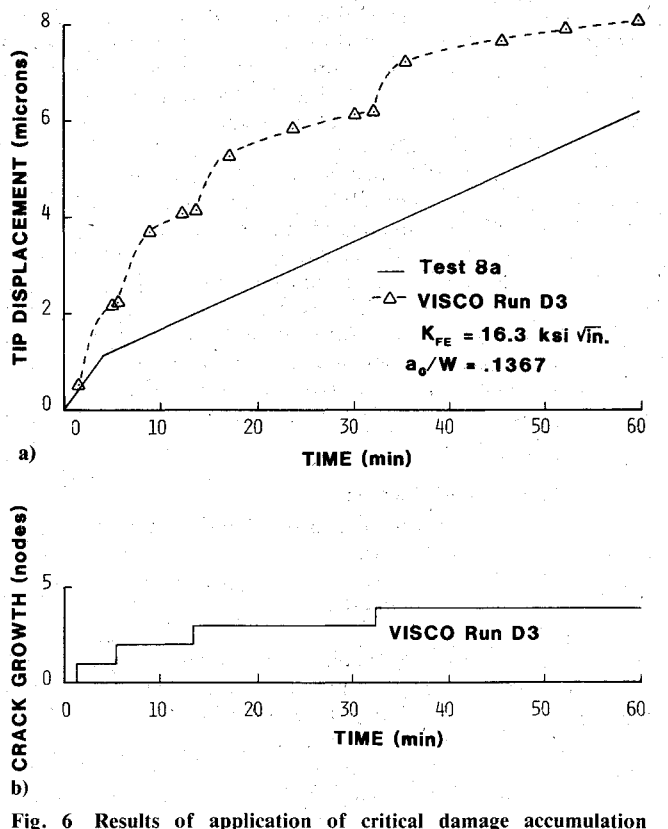

Fig. 6 Results of application of critical damage accumulation criterion, $K=17.9$ MPa$\sqrt{\text{m}}$; a) displacements, b) crack growth.

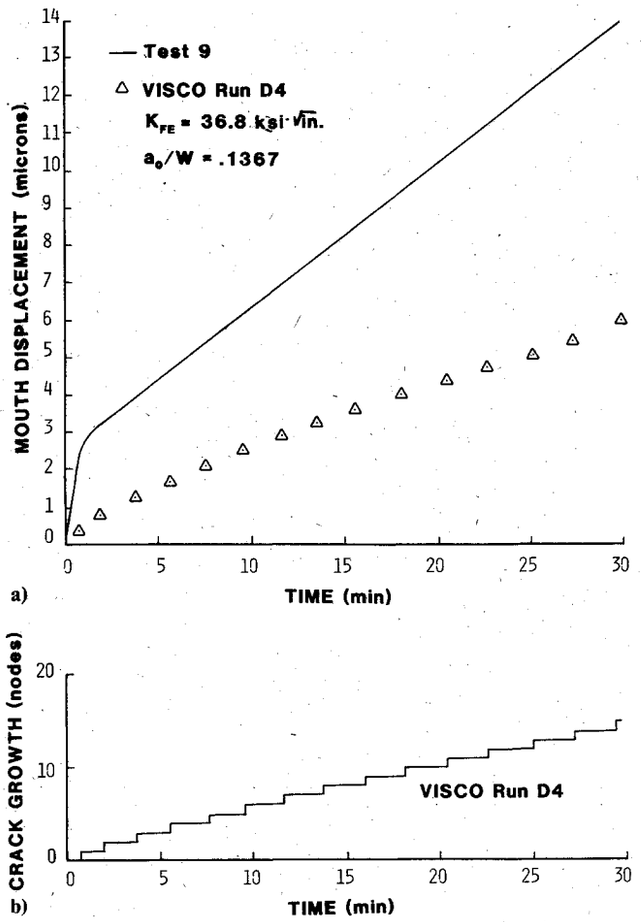

Fig. 7 Results of application of critical damage accumulation criterion, $K = 40.4$ MPa$\sqrt{\text{m}}$; a) displacements, b) crack growth.

order to compare with the lower range of K levels in the current investigation, the line representing the best fit to Donat's data is extrapolated as shown by the dashed line in Fig. 8. Agreement with the present HEN VISCO results, in which K is taken from Table 1 and $\dot{a}$ from the computations using VISCO, is good, especially considering the fact that the test data line is extrapolated.

This criterion has the distinct advantage relative to criteria presented earlier that once the constants A and n are determined, the criterion can be used independent of finite element analyses. This advantage is due to the fact that $\dot{K}$ can be calculated for most test geometries by relatively simple equations which are widely available. Thus the so-called steady-state creep crack growth rate is readily obtained from Eq. (7) for a given loading and test geometry, but neither an incubation time for crack initiation nor the initial rapid crack growth observed in the HEN VISCO results is explainable using this criterion.

B. Net-Section Stress Criterion

Crack growth rates have also been shown to be related to net-section stress in the form

$$\dot{a} = B(\sigma_n)^{\beta} \tag{8}$$

Figure 9 shows how Eq. (8) also is a straight line (the dashed line) on log-log paper. The present results seem to correlate with Eq. (8) as well as they do to Eq. (7) on log-log paper. This result is not surprising because for the center cracked plate it can be shown that K is, approximately, directly proportional to σ_n for crack lengths of a/W from 0.2 to 0.7 which spans the crack lengths in the current study. The net-section stress criterion, like the K criterion, also neglects transient crack growth characteristics.

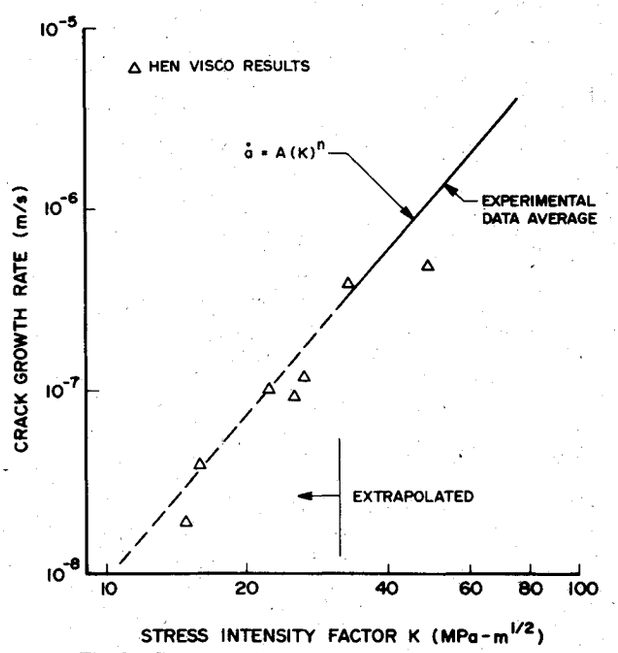

Fig. 8 Crack growth rate vs stress intensity factor.

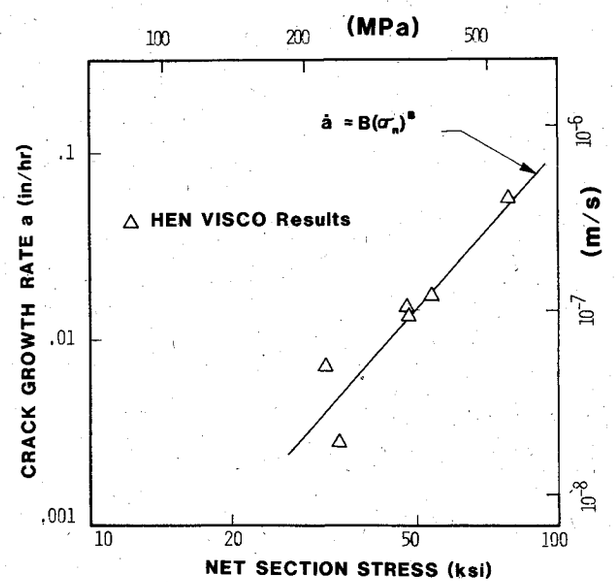

Fig. 9 Crack growth rate vs net-section stress.

C. C^*-Integral Criterion

The C^* integral postulated by Landes and Begley[20] is considered by some to be a better descriptor of slow creep crack growth rate behavior than the linear elastic fracture mechanics stress intensity factor, K, or net section stress. C^* can be determined experimentally fron constant-strain rate tests[20] or constant-load tests[21] by following a step-by-step data reduction scheme. Approximate estimation schemes for C^* have also been developed and compared with the exact value.[22] The C^* integral is obtained directly from the J integral by replacing strain terms by strain rate terms, i.e.,

$$C^* = \int_T \left[W^* \mathrm{d}y - T_i \left(\frac{\mathrm{d}\dot{u}_i}{\mathrm{d}x} \right) \mathrm{d}s \right] \tag{9}$$

where

$$W^* = \int_0^{\dot{\epsilon}_{mn}} \sigma_{ij} \mathrm{d}\dot{\epsilon}_{ij} \tag{10}$$

is the strain energy density rate and dots note differentiation with respect to time. The rationale behind the C^* integral is that, unlike nonlinear elastic material behavior as assumed in the J integral, the behavior of a creeping solid is of the form

$$\dot{\epsilon} = \gamma(\sigma)^{\beta} \tag{11}$$

where γ and β are material constants for a given temperature and environment.

The path independence of the C^* integral can be proven only if the material behavior is described as one of a creeping solid as given by Eq. (11). This implies that a condition of steady-state creep is achieved throughout the body or that stresses are constant. Thus, stress rates are zero as are elastic strain rates. The strain rates in Eqs. (9) and (10) can thus be replaced by the plastic or inelastic portions, assuming that elastic and plastic components are additive. Finally, because constant stresses imply constant strain rates from Eq. (11), the expression for W^*, Eq. (10), can be integrated directly to obtain

$$W^* = \sigma_{ij}\dot{\epsilon}^P_{ij} \tag{12}$$

This expression for W^* is used for all numerical computations of C^*. This approach is taken after several preliminary computations using the exact solution, Eqs. (9) and (10), and clearly demonstrates that the numerical value of C^* depends on the path along which it is evaluated.

In the computations using the approximation, Eq. (12), it is observed that during load application the C^* values are extremely high due to the elastic strain rate contribution. After maximum load is achieved, C^* values reduce to much lower steady-state values until crack growth begins in the HEN VISCO runs. Again, as crack growth begins, the C^* values increase significantly due to the elastic strain rate contribution as stress is redistributing around the moving crack tip. Any attempt to remove elastic contributions to both strain and displacements will result in an ill-posed problem because the displacement rate components needed in Eq. (9) cannot be resolved into an elastic and a plastic portion.

A possibility for evaluating C^* is to ignore the elastic component of strain rate and to calculate it only after the stresses are fairly constant and prior to crack initiation. C^* will then be a constant until the crack begins to grow. Therefore it is impossible to relate C^* to any incubation time for crack growth. Moreover, during crack growth the contribution from elastic strain rates is again substantial and cannot be ignored. Hence, for experimental data in this investigation, it appears that the C^* integral is ineffective as a fracture criterion in a finite element model for creep crack growth over the range of rates covered by this investigation. It should be noted, however, that the crack growth rates encountered here are considerably higher than those usually encountered in creep crack growth experiments. In fact, the sustained load crack growth in the material of this investigation is more typical of stress corrosion cracking behavior than creep crack growth. Thus creep crack growth parameters like C^* should not be expected to correlate the experimental data.

D. Load Point Displacement Rate Criterion

An expression relating crack growth rates to load point displacement rate can be written in the form

$$\dot{a} = B(\dot{\delta})^m \tag{13}$$

Unfortunately this criterion suffers from problems in computations similar to those encountered in the use of the C^* integral. The load point displacement rate, after reaching maximum load, is the sum of the displacement rate due to crack growth as well as the displacement rate due to plastic deformation. Hence, the load point displacement rate can have several values for the same crack growth rate depending on the rate of plastic deformation. One can get an appreciation of how much plastic deformation contributes to the overall displacements by looking at the no-crack-growth displacements vs time. Figure 3 presents the results for test 9 from a computer run (A3) where the crack is not allowed to grow. The plastic deformation is seen to be a measurable fraction of the total deformation, which also includes that due to crack growth. For the cases involving smaller K values, the no-crack-growth plastic deformation is an even larger fraction of the total displacement.[13] The load displacement rate, therefore, does not provide a unique solution to the crack growth rate unless variations in the plastic deformation rate can be neglected.

V. Conclusions

Several parameters obtained from finite element calculations are evaluated for their potential as creep crack growth rate controlling parameters. All calculations are performed using a two-dimensional, plane stress, elastic-plastic computer code developed specifically for this investigation. The results are based on data obtained on center cracked panels of a nickel-base superalloy IN-100, a typical jet engine turbine disk material, tested at 732°C. The numerical approach is felt to be valid for a broad class of materials of this type, which exhibit time-dependent inelastic material behavior. The numerical results support the following conclusions, which are valid only for the material at the specific test temperature.

1) No single fixed value of strain for a critical strain crack growth criterion is found to match all test conditions in this investigation. Environmental effects apparently tend to lower the critical strain magnitude with time, under load. An empirical relationship is developed, based on the HEN results, which gives the critical strain a diminishing value with time and further degrades its value with exposure time at the crack tip. This relationship appears to provide an acceptable approach to defining local failure quantitatively. Due to higher constraint at the crack tip for plane strain, less stress redistribution would occur than in the plane stress case investigated. Therefore it seems possible that the critical strain for all test conditions might vary less in a plane strain simulation than in plane stress.

2) No single fixed value for crack opening displacement (COD) is found to match all test conditions using a critical COD crack growth criterion. This critical COD also degrades with time similar to the crack tip strain; however, its percent variation is less. The calculated displacements are found to be very sensitive to small changes in critical COD, although the critical COD values vary greatly over the range of test conditions.

3) A critical damage accumulation criterion for crack growth is developed based on a modification of the life fraction rule for creep rupture to account for environmental effects at the crack tip. Application of this criterion provides good agreement with the low to medium load test conditions. For the highest load test cases, this criterion predicts crack growth rates somewhat lower than the HEN results. It appears that accumulation of damage over all time and not just crack tip exposure time might improve the results.

4) Data obtained in this investigation through numerical calculations provide crack growth vs time and thus crack growth rate $\dot{a}$. The $\dot{a}$ data compare well with published data for the same material and temperature when plotted against stress intensity factor. The present data are obtained for $\dot{a}$ and K values lower than the referenced data. Net-section stress also provides good correlation with the predicted crack growth rates.

5) The C^* integral and load line displacement rate are investigated as possible parameters controlling crack growth rate $\dot{a}$. The C^* integral is found to be an unreliable parameter

for predicting creep crack growth due to its formulation which is based on a creeping solid behavior that neglects elastic strain rates. The load line displacement rate which can be shown to be proportional to C^* also does not provide a unique solution for the crack growth rate unless variations in plastic deformation rate can be ignored. These two parameters appear to have no applicability to crack growth rate prediction using numerical modeling of materials within the range of growth rates and for the material used in this investigation. On the other hand, these parameters seem to correlate $\dot{a}$ data fairly well once the solution is known, as seen in the literature.

References

[1] Nicholas, T. and Larsen, J. M., "Life Prediction for Turbine Engine Components," Paper presented at 27th Sagamore Army Materials Research Conference, Bolton Landing, N. Y., July 1980; to be published in *Conference Proceedings Fatigue-Environment and Temperature Effects.*

[2] Speidel, M. O., "Fatigue Crack Growth at High Temperatures," *High Temperature Materials in Gas Turbines,* edited by P. R. Sahm and M. O. Speidel, Elsevier Scientific Publishing Company, New York, 1974.

[3] Hinnerichs, T., "Viscoplastic and Creep Crack Growth Analysis by the Finite Element Method," Ph.D. Dissertation, Department of Aeronautics and Astronautics, Air Force Institute of Technology, Wright-Patterson AFB, Ohio, June 1980; see also AFWAL-TR-80-4140, Wright-Patterson AFB, Ohio, July 1981.

[4] Newman, M., Zaphir, F., and Bodner, S. R., "Finite Element Analysis for Time Dependent Inelastic Material Behavior," *Computers and Structures,* Vol. 6, Feb. 1976, pp. 157-162.

[5] Merzer, A. and Bodner, S. R., "Analytical Formulation of a Rate and Temperature Dependent Stress Strain Relations," *Journal of Engineering Materials and Technology, Transactions of ASME,* Vol. 101, July 1979, pp. 254-257.

[6] Bodner, S. R., "Representation of Time Dependent Mechanical Behavior of RENE 95 by Constitutive Equations," AFML-TR-79-4116, Wright-Patterson AFB, Ohio, Aug. 1979.

[7] Bodner, S. R. and Partom, Y., "Constitutive Equations for Elastic-Viscoplastic Strain Hardening Materials," *Journal of Applied Mechanics, Transactions of ASME,* Vol. 42, June 1975, pp. 385-389.

[8] Zienkiewicz, O. C. and Cormeau, I. C., "Visco-Plasticity-Plasticity and Creep in Elastic Solids—A Unified Numerical Solution Approach," *International Journal for Numerical Methods in Engineering,* Vol. 8, Oct. 1974, pp. 821-845.

[9] Armen, H., "Assumptions, Models, and Computational Methods for Plasticity," *Computers and Structures,* Vol. 10, April 1978, pp. 161-174.

[10] Stouffer, D. C., "A Constitutive Representation for IN-100," AFWAL-TR-81-4039, Wright-Patterson AFB, Ohio, June 1981.

[11] Sims, D. L., Annis, C. G. Jr., and Wallace, R., "Application of Fracture Mechanics at Elevated Temperatures," AFML-TR-76-176, Part II, Wright-Patterson AFB, Ohio, April 1977.

[12] Jennings, A., *Matrix Computation for Engineers,* John Wiley and Sons, New York, 1977, Chap. 6, pp. 182-188.

[13] Hinnerichs, T., Nicholas, T., and Palazotto, A., "A Hybrid Experimental-Numerical Procedure for Determining Creep Crack Growth Rates," *Journal of Engineering Fracture Mechanics,* Vol. 16, Feb. 1982, pp. 265-277.

[14] Belie, R. G. and Reddy, J. N., "Direct Prediction of Fracture for Two Dimensional Plane Stress Structures," *Computers and Structures,* Vol. 11, Feb. 1980, pp. 49-53.

[15] Ohtani, R. and Nitta, A., "Crack Propagation in Creep (Experimental Results on Crack Propagation Rates)," *Journal of the Society of Materials Sciences, (Japan),* Vol. 25, No. 275, Aug. 1976, pp. 46-60.

[16] Shahinian, P. and Sadananda, K., "Creep-Fatigue-Environment Interactions on Crack Propagation in Alloy 718," *Engineering Aspects of Creep,* Vol. 2, Institution of Mechanical Engineers, 1980, pp. 1-8.

[17] Goodall, I. W. and Chubb, E. J., "The Creep Ductile Response of Cracked Structures," *International Journal of Fracture,* Vol. 12, No. 2, April 1976, pp. 289-303.

[18] Koterazawa, R. and Mori, T., "Applicability of Fracture Mechanics Parameters to Crack Propagation Under Creep Conditions," *Journal of Engineering Materials and Technology, Transactions of ASME,* Vol. 99, Oct. 1977, pp. 298-305.

[19] Donat, R. C., Nicholas, T., and Fu, L. S., "An Experimental Investigation of Creep Crack Growth in IN-100," presented at the 13th National Symposium on Fracture Mechanics, Philadelphia, June 1980; published in *Fracture Mechanics: 13th Conference,* ASTM STP743, 1981, pp. 186-206.

[20] Landes, J. D. and Begley, J. A., "A Fracture Mechanic's Approach to Creep Crack Growth," in *Mechanics of Crack Growth,* ASTM STP 590, 1976, pp. 128-148.

[21] Sadananda, K. and Shahinian, P., "Creep Crack Growth in Alloy 718," *Metallurgical Transactions, A.,* Vol. 8A, March 1977, pp. 439-449.

[22] Harper, M. P. and Ellison, E. G., "The Use of the C^* Parameter Propagation Rates," *Journal of Strain Analysis,* Vol. 12, July 1977, pp. 167-179.